NJC

Accepted Manuscript

This is an *Accepted Manuscript*, which has been through the Royal Society of Chemistry peer review process and has been accepted for publication.

Accepted Manuscripts are published online shortly after acceptance, before technical editing, formatting and proof reading. Using this free service, authors can make their results available to the community, in citable form, before we publish the edited article. We will replace this *Accepted Manuscript* with the edited and formatted *Advance Article* as soon as it is available.

You can find more information about *Accepted Manuscripts* in the Information for Authors.

Please note that technical editing may introduce minor changes to the text and/or graphics, which may alter content. The journal's standard Terms & Conditions and the Ethical guidelines still apply. In no event shall the Royal Society of Chemistry be held responsible for any errors or omissions in this *Accepted Manuscript* or any consequences arising from the use of any information it contains.

ROYAL SOCIETY OF CHEMISTRY

www.rsc.org/njc

New Journal of Chemistry RSCPublishing

ARTICLE

Synergistic actions between ligand tebuconazole and Cu(II) cation: reasons for the enhanced antifungal activity of four Cu(II) complexes based on fungicide tebuconazole

Cite this: DOI: 10.1039/x0xx00000x

Received 00th January 2012,
Accepted 00th January 2012

DOI: 10.1039/x0xx00000x

www.rsc.org/

Jie Li,[a] Teng Xi,[a] Biao Yan ,[a,b] Yulei Guan,[a] Mingyan Yang,[c] Jirong Song,[a,d] and Haixia Ma*[a]

Abstract: Four Cu(II) complexes, namely, $[CuL_2(SO_4)(DMF)]_n$ **1**, $[CuL_2(CH_3COO)_2]$ **2**, $[CuL_4Cl_2]\cdot 2DMF\cdot 4H_2O$ **3** and $[CuL_4(ClO_4)_2]$ **4**, (**L**=(RS)-1-(4-chloro-phenyl)-4,4- dimethyl-3-(1,2,4-triazole-1-ylmethyl)pentan-3-ol), tebuconazole) have been synthesized, then their structures were identified by elemental analysis (EA), infrared spectra (IR) and single crystal X-ray diffraction (XRD). Moreover, the four obtained complexes were screened for antifungal activities against four selected fungi using mycelial growth rate method. The structural analysis indicates that the different coordination modes of the ligands and counter anions contribute to a one-dimensional polymer chain structure in complex **1** and zero-dimensional mononuclear structures in complex **2**-**4**. The results of the antifungal activities show that all the complexes synthesized show better antifungal activities than the ligand **L**. In addition, the mechanism of the increased antifungal activities of the title complexes in comparison with the ligand was discussed preliminarily and the synergistic interaction between Cu^{2+} and tebuconazole was also investigated by the Wadley approach.

1 Introduction

Plant fungicidal disease is one of the most serious plant diseases and it is also one of the most primary reasons that cause agricultural loss and reductions in seed quality, resulting in the great economic losses.[1] H-1,2,4-Triazole agrochemicals, such as triadimefon, triadimenol, tebuconazole, diniconazole, bitertanol and cyproconazole are a class of biologically significant compounds which were widely used as antifungal agents against mildews and rusts of cereal grains, fruits, vegetables, and ornamentals.[2, 3] These compounds inhibit fungal proliferation by inhibiting steroid demethylation.[4] However, the intensive use of these H-1,2,4-Triazole agrochemicals and their single acting mechanism and active site have led to substantial environmental contamination and a rapid selection of resistance strains.[5-7]

Recently, the complexes, containing transition metal and 1,2,4-triazole ligands have been extensively investigated, mainly because of not only their innovative structures[8-10] but also their application values and development potential in optical, electrical, various biological properties.[11-15] Among these complexes, complexation of pesticides with Cu(II) has potential advantages including the enhancement of persistence, longer shelflife, reduction of mammalian toxicity and conversion of nonsystemic to systemic pesticides.[16-18] Moreover, the pesticides coordinated with transition metals could be utilized as a kind of controlled release formulations which has the capacity of alleviating the toxicity and decreasing the pesticide residue.[19] Meanwhile, the counter anions also show distinct effects during the formation of complexes, not only acting as the charge equilibrium, but also influencing significantly the final structures of the complexes. Different coordination capacity of the counter anions could lead to diversified crystal structures even with the same ligand and metal centers.[20]

In an earlier study, we have reported two Cu(II)complexes of triadimefon and found that the copper complexes exhibited potent antifungal activity toward *Gibberella nicotiancola*, *Gibberella saubinetii*, *Alternaria solani*, *Physalospora berengeriana*, and *Glomerella cingulata*.[21] To continue our work on the complexes of

H-1,2,4-Triazole agrochemicals and to study the impact of counter anions (SO_4^{2-}, CH_3COO^-, Cl^- and ClO_4^-) on the crystal structrues, herein, we report the synthesis, crystal structure and antifungal activity of four Cu(II) complexes of tebuconazole. Interestingly, with variation in anions, complexes were obtained with significant difference in compositions, $[CuL_2(SO_4)(DMF)]_n$ **1**, $[CuL_2(CH_3COO)_2]$ **2**, $[CuL_4Cl_2]$•2DMF•4H_2O **3**, $[CuL_4(ClO_4)_2]$ **4** (**L**=tebuconazole). Even though the crystal structure of the complex of tebuconazole and copper acetate $[CuL_2(CH_3COO)_2]$ **2** (**L**=tebuconazole) has been proposed,[22] its antifungal activities against phytopathogens (selected plant fungi) such as *Gibberella nicotiancola*, *Botryosphaeria berengriana*, *Botryosphaeria ribis* and *Alternaria solani* have not yet been reported, to the best of our knowledge. And the antifungal tests indicate that all of the complexes obtained show superior activities to those of the ligand **L**.

2 Results and discussion

2.1 Synthesis, IR spectroscopy , X-ray powder diffraction and molar conductance

Four Cu(II) complexes, $[CuL_2(SO_4)(DMF)]_n$ **1**, $[CuL_2(CH_3COO)_2]$ **2**, $[CuL_4Cl_2]$•2DMF•4H_2O **3** and $[CuL_4(ClO_4)_2$]**4**, (**L**=tebuconazole) were prepared by the reactions of ligand tebuconazole and a series of copper salts. The fungicide tebuconazole were purchased from commercial source and recrystallized prior to use. The general method employed to prepare the final complexes is outlined in Scheme 1. As shown in scheme 1, reaction of tebuconazole with $CuSO_4$•5H_2O, $Cu(CH_3COO)_{24}$•H_2O led to the mononuclear complex with two ligands, while with $CuCl_2$•2H_2O, $Cu(ClO_4)_2$•6H_2O, generated the mononuclear complex with four ligands. It also can be found that the solvent DMF in complex **1** and **3** present in the crystal lattice, while in complex **2** and **4** the solvent ethanol does not participate in the coordination.

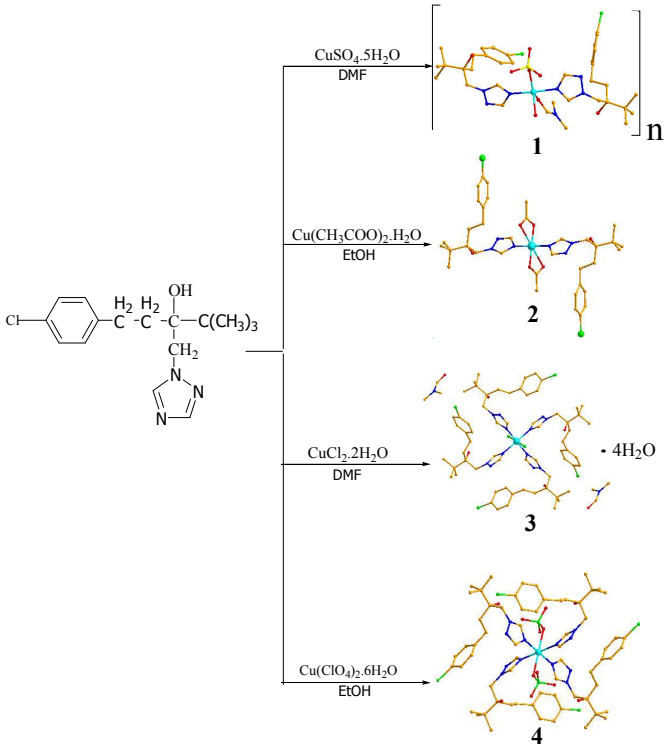

Scheme 1. Formation of copper complexes with tebuconazole.

The IR spectrums of complex **1-4** (Fig. S1 of the ESI†) show that all complexes **1-4** display characteristic bands of alcoholic hydroxyl groups. The alcoholic hydroxyl ν(O–H) stretching vibrations in the IR spectrum of **1-4** are present at 3519, 3251, 3446 and 3441 cm^{-1}, respectively. And there is another ν(O–H) stretching vibration at 3496 cm^{-1} in the IR spectrum of **3**, which should correspond to the ν(O–H) of the lattice waters from complex **3**. The strong absorption bands at 1491-1492 cm^{-1} in the IR spectra of **1-4** are due to the ν(C=C) stretching vibration, respectively. The ν(C–H) stretching vibrations of **1-4** are centered at 3128, 3125, 3122 and 3123 cm^{-1}, respectively. The IR absorption bands at 1648 cm^{-1} of complex **1** and 1680 cm^{-1} of complex **3** are attributed to DMF ν(C=O) mode. This band of complex **1** shifts to lower frequency with respect to that of complex **3** due to the coordination of DMF oxygen to Cu(II), as disclosed from the structural X-ray result. In complex **4**, absorption at 930 cm^{-1} may correspond to ν(Cl–O) of perchlorate. The X-ray powder diffraction patterns are depicted in Fig. S2 of the ESI†. The results show that X-ray powder diffraction patterns of the samples of complex **1-4** are quite similar to the simulated data of the crystal structures, which can prove the bulky phrase of the obtained complexes pure. And Molar conductance values of the complexes **1-4** are 12.6, 1.12, 10.8 and 20.7 S cm^2 mol^{-1}, respectively, in DMF showing them to be non-electrolytes.

2.2 Description of crystal structures

$[CuL_2(SO_4)(DMF)]_n$ 1. X-ray crystal structure analysis of **1** shows that in the asymmetric unit of $[CuL_2(SO_4)(DMF)]$, there is one Cu cation, two **L** ligands, one SO_4^{2-} anion, and one DMF solvent molecule (Fig. 1a). The local coordination geometry around each Cu(II) atom in **1** adopts distorted trigonal bipyramidal geometry, in which each Cu(II) atom is coordinated by two N atoms from two different triazole rings, the bond lengths of Cu-N are in the range of 1.968(4)–1.977(4) Å. The rest coordinated sites are occupied by O atoms: two O atoms from different SO_4^{2-} anions (Cu-O3=1.968(3) Å, Cu-O6=2.073(3) Å) and another from DMF molecule (Cu-O7=2.159(4) Å), suggesting that O3 and O6 atoms are in close

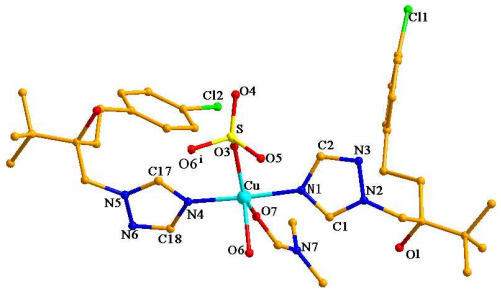

(a)

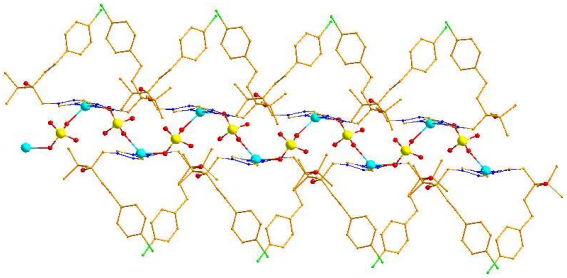

(b)

Fig. 1. Crystal structures of complex **1** (a) coordination mode (symmetry code: [i] 0.5-x, 0.5+y, 0.5-z), hydrogen atoms are omitted for clarity. (b) 1D chain (DMF molecules are omitted for clarity).

contact with Cu atom. The bond angles of N1-Cu-N4, O3-Cu-O6[i] are 174.07(17)º and 130.73(14)º, respectively, which means the coordination sphere of Cu(II) is distorted trigonal bipyramidal. The dihedral angles of benzene ring planes and the attached triazole planes are 82.5° and 72.7°, respectively, so that benzene rings are adjacent to the coordinated triazole planes, resulting in a relatively compact molecule. Each SO_4^{2-} anion is bound to two Cu atoms resulting in the formation of a 1D chain (Fig. 1b). Very intriguingly, the 1D chains display frog-like motifs along the b-axis (Fig. S3 of the ESI†). Furthermore, the 1D chains are connected by Van der Waals force solely to give rise to the 3D framework, as shown in Fig. S4 of the ESI†.

$[CuL_2(CH_3COO)_2]$ 2. The self-assembly of Cu(II) and **L** gave mononuclear $[CuL_2(CH_3COO)_2]$ unit in complex 2. The X-ray structure of **2** shows that the asymmetric unit consists of half Cu(II) atom, one **L** ligand and one CH_3COO^- anion. As shown in Fig. 2a, one N atom from **L** ligand, two O atoms from one CH_3COO^- anion and their symmetric atoms define the distorted octahedral coordination sphere of Cu(II). The Cu-N bond length is 1.966(4) Å, and the bond length of Cu-O2 is 2.625(3) Å, much longer than that of Cu-O3 (1.952(3) Å). The N1–Cu–Ni, O2-Cu-O2[i], and O3-Cu-O3[i] bonds are linearity. The triazole ring plane and its symmetric plane are parallel with a distance of 0.5688 Å. Furthermore, the hydroxyl groups of the ligand forms strong hydrogen bond with coordinated O2 atom on the adjacent $[CuL_2(CH_3COO)_2]$ units (O2…O1[ii] 2.789 Å), thus generating a 1D chain like a zigzag, as shown in Fig. 2b. The adjacent two Cu(II) centers are in a distance of 8.643 Å, suggesting no direct interactions between them.

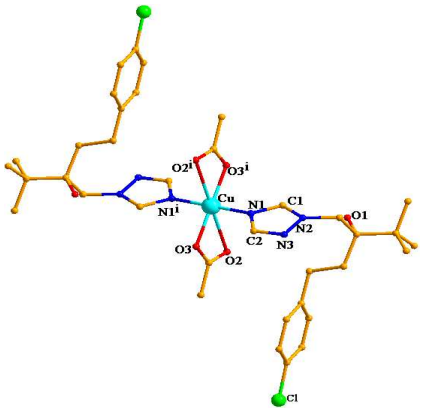

(a)

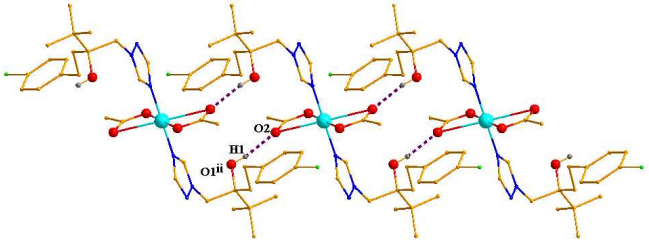

(b)

Fig. 2. Crystal structures of complex **2** (a) coordination mode (symmetry code: [i] 1-x, -y, 1-z), hydrogen atoms are omitted for clarity. (b) 1D chain formed via hydrogen bonds (symmetry code: [ii] -x, -y, 1-z).

$[CuL_4Cl_2]$•2DMF•3H_2O 3. As shown in Fig. 3a, in the symmetric unit of complex **3**, the Cu(II) is octahedrally coordinated to nitrogen atoms from four **L** ligands, chlorine atoms of two Cl^- anions. Whereas, the two DMF and three water solvent molecules do not participate the coordination with Cu(II). The bond lengths of Cu-N are in the range of 1.990(4)–2.031(4) Å, and the bond length of Cu-Cl is 2.764(1) Å, much longer than those of Cu-N, therefore forming an elongated octahedron around the Cu atom. The N1–Cu–N[i], N4–Cu–N4[i], and Cl3-Cu-Cl3[i] bonds are linearity. The triazole ring planes and their symmetric planes are coplanar. The hydrogen bonds between hydroxyl groups of the ligand and coordinated Cl3 atom (O2···Cl3[ii] 3.082 Å) link the unit-cell into a one-dimensional chain (Fig. 3b), with the adjacent Cu···Cu contact of 8.139 Å, which excludes any metal–metal interaction.

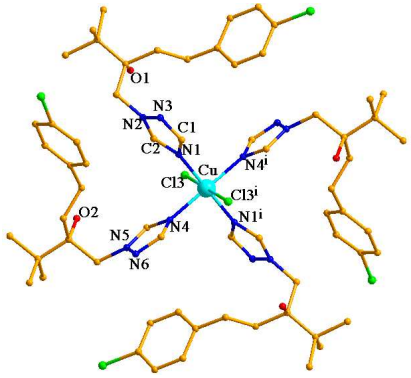

(a)

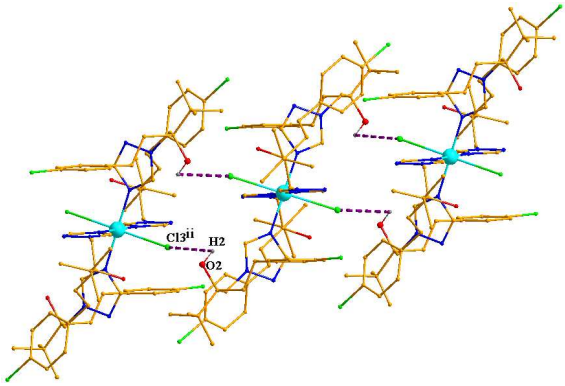

(b)

Fig. 3. Crystal structures of complex **3** (a) coordination mode (symmetry code: [i] 1-x, -y, -z), hydrogen atoms are omitted for clarity. (b) 1D chain formed via hydrogen bonds (symmetry code: [ii] 1-x, y, 1.5-z). Solvents are omitted for clarity.

$[CuL_4(ClO_4)_2]$ 4. As given in Fig. 4a, complex **4** has a similar structure to that of complex **3**, with two ClO_4^- anions instead of Cl^- anions coordinated to Cu(II) center and without solvent molecules. In complex **4**, the Cu–O bond length is 2.583(3) Å and Cu–N distances are in the range of 1.989(3)–2.017(3) Å, which are all in good agreement with those in the above three complexes. Whereas, complex 4 has the biggest Cu···Cu distance (9.713 Å). The N1–Cu–N[i], N4–Cu–N4[i], and O2-Cu-O2[i] bonds are all linear. The triazole ring planes and their

symmetric planes are parallel with distances of 0.2207 Å and 0.4720 Å, respectively. The hydroxyl groups of the ligand forms strong hydrogen bond with O5 and O6 atoms from perchlorate groups on two adjacent molecules (O2···O5^{ii} 2.850 Å, O1···O6^{iii} 3.155 Å) link the unit-cell of [Cu**L**$_4$(ClO$_4$)$_2$] **4** into a one-dimensional chain (Fig. 2b). Crystal data and structure refinement details are summarized in Table1. Selected bond lengths and angles are listed in Table 2.

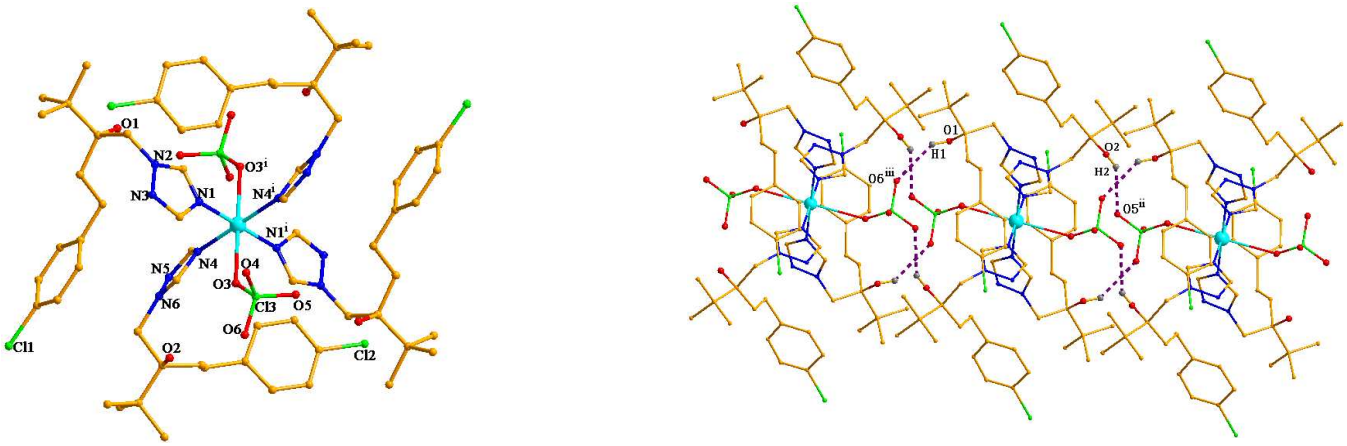

Fig. 4. Crystal structures of complex **4** (a) coordination mode (symmetry code: ^{i} 1-x, 1-y, 1-z), hydrogen atoms are omitted for clarity. (b) 1D chain formed via hydrogen bonds (symmetry code: ^{ii} 1+x, y, z; ^{iii} -x, 1-y, 1-z).

Table 1. Crystallographic data for complex **1-4**

complex	**1**	**2**	**3**	**4**
Empirical formula	$C_{35}H_{51}Cl_2CuN_7O_7S$	$C_{36}H_{50}Cl_2CuN_6O_6$	$C_{70}H_{108}Cl_6CuN_{14}O_9$	$C_{64}H_{88}Cl_6CuN_{12}O_{12}$
Formula weight	848.33	797.26	1583.96	1493.70
Cryst system	monoclinic	monoclinic	monoclinic	triclinic
Space group	*C*2/*c*	*P*21/n	*C*2/*c*	*P*-1
a / (Å)	30.652(5)	8.643(3)	25.8681(18)	9.713(2)
b / (Å)	8.830(15)	21.583(8)	19.8556(18)	13.623(3)
c / (Å)	30.761(5)	11.460(4)	16.2770(13)	15.213(3)
α / (°)	90.00	90.00	90.00	65.309(2)
β / (°)	108.628(3)	107.229(7)	101.368(2)	84.320(2)
γ / (°)	90.00	90.00	90.00	79.878(2)
V /(Å^3)	7890(2)	2042.1 (12)	8196.3 (11)	1799.7(6)
Z	8	2	4	1
D_c (g·cm^{-3})	1.428	1.297	1.269	1.378
F(000)	3560	838	3316	783
Reflcns collcd	20719	11023	20293	11057
Unique/observed	7796/4464	4194/2416	7811/3513	6049/4810
R_{int}	0.0800	0.0726	0.0579	0.1094
GOF	0.975	0.971	1.242	1.075
*R*1(I≥2σ(I))	0.0612	0.0635	0.0717	0.0527
*wR*2 (I≥2σ(I))	0.1536	0.1545	0.1472	0.1462

Table 2. Selected bond lengths (Å) and angles (º) for complex **1**-**4.**

Complex **1**		Complex **2**		Complex **3**		Complex **4**	
Cu-N1	1.977(4)	Cu-N1	1.969(3)	Cu-N1	1.990(4)	Cu-N1	1.989(3)
Cu-N4	1.968(4)	Cu-N1^{i}	1.969(3)	Cu-N1^{i}	1.990(4)	Cu-N1^{i}	1.989(3)
Cu-O3	1.968(3)	Cu-O2	2.625(3)	Cu-N4	2.031(4)	Cu-N4	2.017(3)
Cu-O6	2.073(3)	Cu-O2^{i}	2.625(3)	Cu-N4^{i}	2.031(4)	Cu-N4^{i}	2.017(3)
Cu-O7	2.159(4)	Cu-O3	1.952(3)	Cu-Cl3	2.764(1)	Cu-O2	2.583(3)
N1-Cu-N4	174.07(17)	Cu-O3^{i}	1.952(3)	Cu-Cl3^{i}	2.764(1)	Cu-O2^{i}	2.583(3)
O3-Cu-O6	130.73(15)	N1-Cu-N1^{i}	180.0	N1-Cu-N1^{i}	180.0	N1-Cu-N1^{i}	180.0
N1-Cu-O3	89.52(15)	O2-Cu-O2^{i}	180.0	N4-Cu-N4^{i}	180.0	N4-Cu-N4^{i}	180.0
N1-Cu-O6	88.32(14)	O3-Cu-O3^{i}	180.0	Cl3-Cu-Cl3^{i}	180.0	O2-Cu-O2^{i}	180.0
N4-Cu-O3	90.03(15)	N1-Cu-O2	90.23(12)	N1-Cu-N4	90.40(16)	N1-Cu-N4	89.00(12)
N4-Cu-O6	96.42(15)	N1-Cu-O3	90.52(13)	N1-Cu-N4^{i}	89.60(13)	N1-Cu-N4^{i}	91.00(12)

Symmetry codes: Complex **2** ^{i}1-x, -y, 1-z. Complex **3** ^{i}1-x, -y, -z. Complex **4** ^{i}1-x, -y, -z.

2.3 Biological activities

2.3.1 Antifungal activities

Based on antifungal screening data (Table 3), generally, the antifungal activities of the metal complexes synthesized show remarkable inhibitory effects on selected plant pathogenic fungi: they were all more active than the ligand **L**, which is a highly effective fungicide and widely used on the market. Among the four title complexes, complex **3** and **4** show better inhibitory activities against the tested fungi, especially complex **3** exhibits the best activities. And for *A. Solani*, all the obtained complexes show the greatest toxicity ratios(4.72, 7.22, 14.16 and 8.63, respectively) in comparison with **L.**

Table 3. EC_{50} values of **L** and their metal complexes against plant pathogenic fungi (μM).

compound	*G.nicotian cola*	*B.berengri ana*	*B.ribis*	*A.solani*
1	2.01	6.10	0.44	0.75
2	1.94	7.34	0.76	0.49
3	1.25	3.19	0.30	0.25
4	1.30	4.63	0.33	0.41
L	2.50	11.9	1.75	3.54
$CuSO_4$	44.6	44.4	32.4	63.9
$Cu(CH_3COO)_2$	44.5	44.7	32.5	64.7
$CuCl_2$	44.1	44.4	32.0	64.3
$Cu(ClO_4)_2$	45.0	44.6	32.2	63.8

The bioassay of the metal salts showed that the salts of $CuSO_4$, $Cu(CH_3COO)_2$, $CuCl_2$ and $Cu(ClO_4)_2$ have a certain degree of antifungal effect (Table 3). We found that the fungicidal activities of the four inorganic copper salts against the same selected fungi did not exhibit obvious diversity; this result indicated that the bioactivities of the title complexes were related to only the synergistic action of the ligand and metal cation, substantively irrelative to the anions. Therefore, it was the coordinating of the ligand and the Cu cation that increased the bioactivities. This

conclusion is consistent with that found in our previous work.[21] Such increased activity of the metal complexes can be explained on the basis of chelation theory. On chelation, the polarity of the metal cation will be reduced to a great extent due to the overlap with the ligand orbital. Further, it increases the delocalization of π-electrons over the whole chelate ring and enhances the lipophilicity of the complexes.[23, 24]

2.3.2 Synergistic interaction between Cu^{2+} and tebuconazole

Fig. 5 shows the interaction between Cu^{2+} and tebuconazole. For the molecular-level mixture of Cu^{2+} and tebuconazole tested against the four selected fungi, all the interaction levels were synergistic, since all the SR are more than 1.5 (the minimum SR is 1.82). The maximum synergy level reached 10.40 for complex **3** against *A. solani*. Moreover, the interaction levels of complex **3** and **4** were higher than those of complex **1** and **2** for the same tested fungus, which indicates that synergy levels are strongly dependent on the ratio of the components in the mixture, and here the synergy levels were better for the ratio 1:4 of molecular-level mixture of Cu^{2+} and tebuconazole than those for the ratio 1:2. It is also found that any synthesized complex show different synergy levels to the tested fungi, and the synergy levels sequence concerning the tested fungi is *A. solani* > *B. ribis* > *B. berengriana* > *G. Nicotiancola*, which indicates the complexes might share various action modes with the tested fungi. However, to prove this possibility, further chemical and biological investigation is needed to clarify action mechanisms of these obtained complexes.

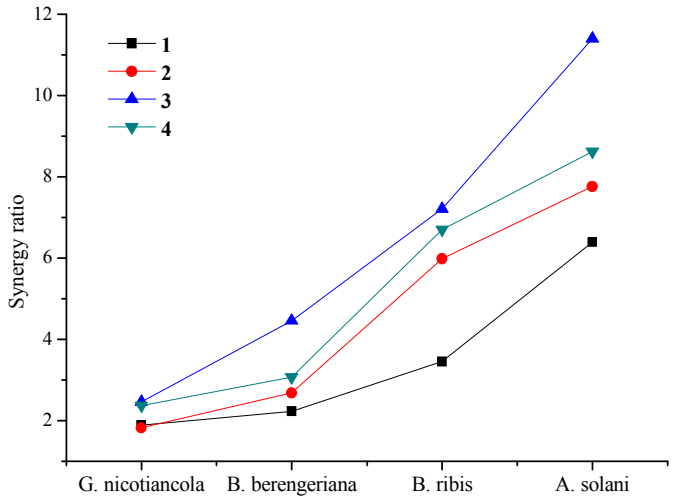

Fig. 5. Interaction (SR) between Cu^{2+} cation and tebuconazole.

3 Conclusions

Four Cu(II) complexes from ligand tebuconazole have been prepared and identified with structures of 1D polymer chain in complex **1** and 0D mononuclear coordination mode in complex **2-4**. The antifungal activity tests show that all the obtained complexes are more efficient to inhibit the four selected plant pathogenic fungi than the ligand tebuconazole, which show potential applications of these complexes in the fields of antifungal agents. Further, it is found that the bioactivities of the obtained complexes were related to only the synergistic action of the ligand and metal cation, substantively irrelative to the anions. And the investigation of the synergistic interaction between Cu^{2+} and tebuconazole reveal that the synergy levels for the ratio 1:4 of molecular-level mixture of Cu^{2+} and tebuconazole are better than that for the ratio 1:2. And the synergy levels sequence concerning the tested fungi is *A.solani* > *B.ribis* > *B.berengriana* > *G. Nicotiancola*.

4 Experimental Section

4.1 Materials and general methods

Tebuconazole was purchased from commercial source and recrystallized by isopropyl alcohol solvent. The melting point of the purified tebuconazole is measured as 102.1-104.0 °C. IR (KBr, σ/cm^{-1}): 3300 (m), 3140 (w), 2973 (s), 2876(w), 1510 (vs), 1490(vs), 1009(s). All other reagents were of reagent grade and used as received. Elemental analysis was performed on a Vario EL III elemental analyzer. IR spectrum was carried out on EQUINX 55 with KBr presser bit. X-ray diffraction data were collected on a Bruker SMART APEX CCD diffractometer. Powder X-ray diffraction (PXRD) patterns were measured on a Bruker D8 Advance X-ray powder diffractometer with Cu Kα radiation (λ=0.15405 nm). Conductances were measured in 10^{-3} M DMF on a DDS-11A model cinductivity meter. Melting points were recorded on a Tech X-5 model hot-stage microscope.

4.2 Synthesis of the complexes

$[CuL_2(SO_4)DMF]_n$ **1**: the copper sulfate pentahydrate (0.1249 g, 0.5 mmol) was dissolved in DMF (3 ml), at the same time, tebuconazole (0.6156 g, 2 mmol) was dissolved in DMF (5 ml). The above two solutions were mixed and stirred at room temperature. After 4 h, the resulting solution remained completely clear, thereafter the solution was kept at room temperature for slow evaporation. 15 days later, single crystals suitable for single crystal X-ray analysis were obtained by slow evaporation. Yield: 63%. Elemental analysis calcd (%) for $C_{35}H_{51}Cl_2CuN_7O_7S$ (Mr = 848.33): C 49.55, H 6.06, N 11.56; found: C 48.96, H 6.15, N l1.88. IR (KBr, σ/cm^{-1}): 3519 (m), 3128 (w), 2965 (m), 2876(w), 1648(s), 1531 (s), 1492 (s), 1015(m).

$[CuL_2(CH_3COO)_2]$ **2**: A solution of tebuconazole (0.6156 g, 2 mmol) in methanol (10 mL) was added drop wise to a solution of copper acetate monohydrate (0.1997 g, 1 mmol) in methanol (5 mL) medium. The resulting mixture was refluxed for 3 h to give a clear solution, and then cooled to room temperature. Upon slow evaporation, blue crystals were obtained at room temperature after 6 days. Yield: 86%. Elemental analysis calcd (%) for $C_{36}H_{50}Cl_2CuN_6O_6$ (Mr = 797.26): C 54.23, H 6.32, N 10.54; found: C 54.56, H 6.25, N l0.83. IR (KBr, σ/cm^{-1}): 3251 (m), 3125 (w), 2967 (m), 2876(w), 1532 (w), 1492 (m), 1016(m).

$[CuL_4Cl_2]$•2DMF•$3H_2O$ **3**: This mononuclear complex was prepared by following essentially the same procedure for the preparation of complex **1**, except that copper chloride dihydrated was used instead of copper sulfate pentahydrate. Yield: 65%. Elemental analysis calcd (%) for $C_{70}H_{108}Cl_6CuN_{14}O_9$ (Mr = 1565.94): C 53.69, H 6.95, N 12.52; found: C 52.94, H 6.68, N l2.22. IR (KBr, σ/cm^{-1}): 3496 (m), 3446 (m), 3122 (m), 2967 (s), 2876(w), 1680(s), 1521 (s), 1491 (vs), 1018(s).

$[CuL_4(ClO_4)_2]$ **4**: This complex was prepared by following essentially the same procedure for the preparation of complex **2**, except that perchlorate hexahydrate was used instead of copper acetate monohydrate, yield: 52%. Elemental analysis calcd (%) for $C_{64}H_{88}Cl_6CuN_{12}O_{12}$ (Mr = 1493.70): C 51.46, H 5.94, N 11.25;

found: C 51.96, H 6.02, N l1.38. IR (KBr, σ/cm^{-1}): 3441 (m), 3123 (m), 2965 (m), 2876(w), 1528 (w), 1491 (m), 1010(m), 930(m).

4.3 Crystal structure determination

Single-crystal X-ray diffraction (XRD) measurements of the four obtained complexes were carried out on a Bruker SMART APEX CCD diffractometer equipped with a graphite monochromator using Mo Kα radiation (0.71073 Å) at 296(2) K in the *φ*-*ω* scan mode. Unit cell dimensions were obtained with least-squares refinements and semi-empirical absorption corrections were applied using the SADABS program.[25] The structure was solved by direct methods and refined by full-matrix least squares techniques based on F^2 with the SHELXTL-97 program.[26] All non-hydrogen atoms were obtained from the difference Fourier map and refined with atomic anisotropic thermal parameters. H atoms bonded to C and hydroxy O atoms were placed at calculated positions and refined using a riding-model approximation with U_{iso}(H) = 1.5U_{eq}(C) for methyl and hydroxy H atoms and 1.2 *U*eq(C) for other H atoms. In complex **3**, H atoms bonded to water O atoms were located in a difference Fourier maps and treated as riding atoms, with U_{iso}(H) = 1.5U_{eq}(O). Crystallographic data for structures **1**-**4** have been deposited at the Cambridge Crystallographic Data Centre as supplementary publication CCDC 934449, 934442, 934438 and 1421333.

4.4 Biological activities tests

Four important phytopathogens (*Gibberella nicotiancola*, *Botryosphaeria berengriana*, *Botryosphaeria ribis* and *Alternaria solani*) were provided by Shaanxi Microbiology Institute, China, and they were selected for antifungal activity studies. The antifungal activities of ligand **L**, the title complexes and the metal salts $CuSO_4$, $CuCl_2$, $Cu(CH_3COO)_2$ and $Cu(ClO_4)_2$ were carried out by mycelial growth rate method.[21, 27, 28] Sterilized PDA was cooled to 50 °C and mixed well with these target compounds to obtain a range of concentrations (1, 2, 4, 8 μmol/L) immediately before pouring into the petri plates (7.5 cm in diameter). The prepared phytopathogens were inoculated in each well of 8 mm diameter (made with a borer), and then the fungi strains were cultured at 28 °C for 72 h. Petri plates inoculated with the fungal strains without any compound were also incubated as control. Each experiment was performed in triplicate. The diameter of fungal colonies on PDA plates was measured after 72 h. Percentage inhibition of mycelial growth was calculated using formula (1). Because the synthesized complexes can be regarded as the molecular-level mixtures of **L** and inorganic copper salts, synergy ratios (SR) were calculated to investigate the extent of the interactions between **L** and inorganic copper salts according to Wadley approach[29] using formulas (2) and (3).

$$\%\text{Inhibition}=\frac{(\text{Colony diameter of control})-(\text{Colony diameter of compound})}{\text{Colony diameter of control}} \quad (1)$$

$$EC_{50}(\text{expected})=(a+b)/[(a/EC_{50A})+(b/EC_{50B})] \quad (2)$$

$$SR=EC_{50}(\text{expected})/EC_{50}(\text{observed}) \quad (3)$$

where A, B are two antifungal components; a, b indicate the ratios of A and B to the complex, respectively: If SR≤0.5, the level of interaction of single components in complex is antagonistic; if 0.5>SR<1.5, the level is additive; if SR≥1.5, the level is synergistic.

Acknowledgements

This work is funded by the National Natural Science Foundation (21373161), New Century Excellent Talents in University of Ministry of Education of China (NCET-12-1047), Research Fund for the Doctoral Program of Higher Education of China (RFDP, No. 20126101110009).

Notes

[a] *School of Chemical Engineering, Northwest University /Shaanxi Key Laboratory of Physico-Inorganic Chemistry, Xi'an, Shaanxi 710069, China. Tel./fax: +86-029-88307755; E-mail: mahx@nwu.edu.cn*
[b] *Department of Chemistry and Chemical Engineering, University of Yulin, Yulin, Shaanxi, 719000, China.*
[c] *Department of Environmental Science and Engineering, Chang'an University, Xi'an, Shaanxi 710054, China.*
[d] *Conservation Technology Department, the Palace Museum, Beijing 100009, China.*
† Electronic Supplementary Information (ESI) available: CCDC 934449 **1,** 934442 **2**, 934438 **3** and 1421333 **4**. For ESI and crystallographic data in CIF or electronic format see DOI: 10.1039/b000000x/

References

1 J.E. Benett, Goodman and Gilman's, *The pharmacological basis of the rapeutics*, McGraw-Hill Inc, New York, 1995.
2 M.G. Cromey, R.C. Butler, M.A. Mace and A.L.J. Cole, *Crop Prot.*, 2004, **23**, 1019- 1030.
3 PJ. Cotterill, *Crop Prot.*, 1993, **12**, 273- 278.
4 M. Gasztonyi and G. Josepovits, *Pestic. Sic.*, 1979, **10**, 57- 65.
5 J.A. Zarn, B.J. Brschweiller and J.R. Schlatter, *Environ. Health Perspect.*, 2003, **111**, 255-261.
6 S. Pille and M. Koppel, *Agr. Food Sci*., 2010, **19**, 34-42.
7 J. Fan, F. Chen, Y. Diao, H.J. Cools, S.L. Kelly and X. Liu, *Plant Pathol.*, 2014, **63**, 952-960.
8 V.B. Arion, E. Reisner, M. Fremuth, M.A. Jakupec, B.K. Keppler, V.Y. Kushkin and A.J.L. Pombeiro, *Inorg. Chem*, 2003, **42**, 6024-6031.
9 P.P. Xiong, J. Li, H.Y. Bu, Q. Wei, R.L. Zhang and S.P. Chen, *J. Solid State Chem.*, 2014, **215**, 421-435.
10 X.R. Meng, Y.L. Song, H.W. Hou, H.Y. Han and B. Xiao, *Inorg. Chem.*, 2004, **43**, 3528-3536.
11 J. Li, P.P. Xiong, H.Y. Bu and S.P. Chen, *Acta Phys-Chim Sin.*, 2014, **30**, 1354-1362.
12 N. Boechat, V.F. Ferreira, S.B. Ferreira and M.L.G. Ferreira, *J. Med. Chem.*, 2011, **54**, 5988-5999.
13 J. Aguiló, A. Naeimi, R. Bofill, H. Mueller-Bunz, A. Llobet, L. Escriche, X. Sala and M. Albrecht, *New J. Chem.*, 2014, **38**, 1980-1987.
14 J.M Liu, L. Wang, K. Yu, Z.H. Su, C.X. Wang, C.M. Wang and B.B. Zhou, *New J. Chem.*, 2015, **39**, 1139-1147.

15 Y.H. Wang, D.Y. Yu, P. Xu, B.Y. Guo, Y.F. Zhang, J.Z. Li and H.L. Wang, *Ecotox. Environ. Safe.*, 2014, **107**, 276-283.
16 A.K. Sadana, Y. Mirza, K.R. Aneja and O. Prakash, *Eur. J. Med. Chem.*, 2003, **38**, 533-536.
17 M. Kamiya and K. Kameyama, *Chemosphere*, 2001, **45**, 231-235.
18 E. Morillo, T. Undabeytia, C. Maqueda and A. Rams, *Chemosphere*, 2002, **47**, 747-752.
19 P.Z. Zhang, Q.Y. Fu, R.X. Chi, C.X. Yang and J.G. Xu, *J. Zhejiang Univ. Sci. Technol.,* 2003, **15**, 142-145.
20 M. Du and X.H. Bu, *J. Inorg. Chem.*, 2003, **19**, 1-5.
21 J. Li, T. Xi, B. Yan, M.Y. Yang, J.R. Song and H.X. Ma, *New J. Chem.*, 2015, DOI: 10.1039/c5nj00679a.
22 P.D. Evans and K.J. Schmalzl, *J. Wood Chem. Technol.*, 2007, **27**, 243-256.
23 A. Chaudhary, N. Bansal, A. Gajraj and R.V. Singh, *J. Inorg. Biochem.*, 2003, **96**, 393-400.
24 K.Y. El-Baradie, *Monatshefte für Chem.*, 2005, **136**, 1139-1155.
25 G.M. Sheldrick, *SADABS,* University of Göttingen, Germany, 2000.
26 G. M. Sheldrick, *Acta Crystallogr. Sect. A*, 2008, **64**, 112-122.
27 D. Saetae and W. Suntornsuk, *J. Microbiol. Biotechnol.*, 2010, **20**, 319-324.
28 R.K. Devappaa, S.K. Rajeshb and V. Kumara, *Ecotoxicol. Environ. Saf.*, 2012, **78**, 57-62.
29 F.M. Wadley, *Experimental statistics in entomology*, Graduate School Press, Washington State University, Pullman, 1976.

The enhanced antifungal activity of four synthesized complexes are due to the synergistic actions of ligand tebuconazole and Cu(II) cation.